3 Biotech (2020) 10:446
https://doi.org/10.1007/s13205-020-02432-w

ORIGINAL ARTICLE

AuNPs/CNF-modified DNA biosensor for early and quick detection of *O. tsutsugamushi* in patients suffering from scrub typhus

Deepak Kala[1] · Tarun Kumar Sharma[3] · Shagun Gupta[2] · Rupak Nagraik[2] · Vivek Verma[2] · Atul Thakur[1] · Ankur Kaushal[1]

Received: 6 July 2020 / Accepted: 8 September 2020 / Published online: 19 September 2020

Abstract

A novel approach has been developed for the detection of *56 kDa tissue-specific antigen* (TSA) gene of *Orientia tsutsugamushi* a causative agent of scrub typhus disease. The approach was developed by immobilization of 5′ NH2 labeled ssDNA probe selective *to 56 kDa TSA* gene, to the surface of AuNPs/CNF modified screen-printed electrode. An electrochemical response was recorded with single stranded genomic DNA (ssDNA) of *O. tsutsugamushi* isolated from patient sample, using cyclic voltammetry and electrochemical impedance spectroscopy. The electrode surface was characterized by Field-Emission Scanning electron microscope (FE-SEM), Fourier Transform Infrared Spectroscopy (FTIR) and Raman Spectroscopy at each step of fabrication. The DNA biosensor shows optimum response within 50–60 s at room temperature (25 ± 3 °C). The sensor shows higher sensitivity [7849 (μA/cm^2)/ng DNA], fast response time (60 s), wider linear range (0.04–2.6 ng) with limit of detection of 0.02 ng/μl of ssDNA sample.

Keywords DNA biosensor · Scrub typhus · *Orientia tsutsugamushi* · Carbon nanofibers · Electrochemical DNA sensor

Introduction

Scrub typhus is a zoonotic infection caused by intracytosolic, Gram negative bacterium *Orientia tsutsugamushi,* resulting in an acute febrile illness and indigenous to 'tsutsugamushi triangle' (Paris et al. 2013; Prakash 2017). Human is an incidental, dead-end host, transferred by the bite of infected parasitic larval stage of the mite *Leptotrombidium deliense* (Shivalli 2016). The disease is highly prevalent in rural areas of Southeast Asia including India, Thailand, Korea, Australia, Russia, The Pacific Islands and Japan (Saraswati et al. 2018). Scrub typhus cases accounts for up to 23% of all febrile illnesses, with an estimated case occurrence of one million each year, in endemic areas (Chunchanur 2018). The fatality rate of scrub typhus can reach 30% or even higher in the lack of appropriate treatment (Xu et al. 2017). Coinciding symptoms of scrub typhus with other co-endemic diseases such as leptospirosis, dengue and typhoid makes it difficult to distinguish (Bonell et al. 2017). Presence of eschar in mite biting site is a specific (98.9%) marker used for clinical diagnosis of scrub typhus; however, the presence of eschar is varied widely in patients from 7 to 97% (Lee et al. 2009). The laboratory-based diagnosis of scrub typhus relies on serological assays like weil-felix

Electronic supplementary material The online version of this article (https://doi.org/10.1007/s13205-020-02432-w) contains supplementary material, which is available to authorized users.

✉ Ankur Kaushal
akaushal@ggn.amity.edu

Deepak Kala
deepakbiotech90cu@gmail.com

Tarun Kumar Sharma
tarun@thsti.res.in

Shagun Gupta
shagungupta@shooliniuniversity.com

Rupak Nagraik
rupaknagraik@shooliniuniversity.com

Vivek Verma
vivek77verma@gmail.com

Atul Thakur
athakur1@ggn.amity.edu

[1] Amity Center of Nanotechnology, Amity University, Haryana 122413, India

[2] Shoolini University, Solan 173229, India

[3] Translational Health Science, and Technology Institute, Faridabad 121001, India

test, indirect immunofluorescence assay, indirect immunoperoxidase assay, ELISA and immunochromatographic tests (ICT) etc. Among all serological assays, IFA and ELISA-based method is most reliable for detection of scrub typhus (Xu et al. 2017). Immuno-based methods required paired sampling for confirmation of scrub typhus as standard cut-off value for antibody titer has not yet defined and varied among different studies conducted in endemic areas (Saraswati et al. 2019). Due to retrospective approach, paired sampling-based methods become unsuitable for early-stage diagnosis of scrub typhus. On the other hand, molecular assays rely on PCR-based diagnosis of scrub typhus with more specificity and sensitivity using eschar and blood samples. However, genetic variations among strains of *O. tsutsugamushi* and lower recovery of DNA from patients' blood sample are the biggest challenge for its diagnosis using PCR. More than 20 antigenically distinct strains have been identified till now that includes 3 prototypic strains Karp, Kato and Gilliam. Antigenic variations among strains have been linked to highly diverse *56-kDa TSA* immunodominant gene, specific to *O. tsutsugamushi* (Koh et al. 2010; Phetsouvanh et al. 2013; Kelly et al. 2009; Lin et al. 2011). It encodes a primary immunogen (type-specific antigen) located on the outer membrane surface of *O. tsutsugamushi* and responsible for eliciting neutralizing antibodies (Blacksell et al. 2008). Apart from *56 kDa TSA* gene, few other genes have also been identified as genetic markers including 47-kDa high temperature requirement A (*HtrA*) and 16S *rRNA* gene etc. (Rodkvamtook et al. 2011; Yang et al. 2012). Among all *56 kDa TSA* is most widely used genetic marker for detection of scrub typhus due to its well studied genetic variations among serotypes of *O. tsutsugamushi* (Kala et al. 2020; Premaratna et al. 2017; Biswal et al. 2018; Usha et al. 2016; Zheng et al. 2015; Zhang et al. 2015; Varghese et al. 2015; Usha et al. 2015).

These days DNA-based biosensors have become new advanced diagnostic tools and are highly sensitive and specific for their target sites (Singh et al. 2017a, b; Kaushal et al. 2016). They can become future of disease diagnosis especially for the diseases like scrub typhus, which is having issues of specificity and sensitivity. Furthermore, sensitivity of biosensors can be improved by modification with nanomaterials and nanocomposite that improves sensitivity of sensor and provide more surface area for immobilization of bioreceptors. Recently several advanced nanostructured carbon materials like MWCNT, SWCNT, graphene, and carbon nanofibers (CNF) have been employed for construction of biosensors due to their better electrocatalytic activity than traditional carbon materials (Li et al. 2007, Wu et al. 2010, Baby et al. 2010, Zhou et al. 2008). Among all nanostructured carbon materials, carbon nanofibers (CNF) have received much attention due to their larger surface area, thermal and mechanical stability with low ohmic resistance (Wang et al. 2012). The CNFs and CNTs are similar in terms of several properties like mechanical strength and electric properties but the advantage of CNFs is that its graphite ordering can be controlled and stacking of various size graphene sheets in its structure produces more edge plane that may facilitate the electron transfer of electroactive species. CNFs have a unique property that its whole surface area can be activated, which provides a much larger functionalized surface area. These properties make CNFs an ideal platform for immobilization of biomolecules and a better transducer (Huang et al. 2010). Unique properties of gold nanoparticles (AuNPs) such as good conductivity and nano-scaled dimension effect received much interest for preparing composite with other nanomaterials in the fabrication of sensors (Song et al. 2011; Hu et al. 2011; Wang et al. 2010; Ulianas et al. 2014). The biocompatibility of AuNPs aid to maintain the bioactivity of immobilized biomolecules and its higher surface-area-to-volume ratio enhances the electron transfer kinetics on the transducer surface (Lin et al. 2015). Gold nanoparticles in combination with other carbon nanomaterials have already been deployed for construction of biosensors for detection of analytes in biological samples (Table 1). However, only few studies have reported the use of AuNPs

Table 1 Comparison of different types of carbon nanomaterials and nanocomposites based DNA sensor

S. n.	Type of sensor	Target Analyte	Sensing material	Sensitivity	Reference
1.	Amperometric DNA sensor for bacterial meningitis	*rmpM* gene	Carbon-MOD/MWCNT	3.762 (μA/cm^2)/ng	Dash et al. (2014)
2.	Amperometric DNA sensor for RHD	*Mga gene*	Carboxylated MWCNT	106.03 (μA/cm^2)/ng	Singh et al. (2014)
3.	Amperometric DNA sensor	*speB* gene	Nano-Au/cMWCNT	104.7 μA cm^{-2} ng^{-1}	Kaushal et al. (2017)
4.	Amperometric DNA sensor for leptospirosis	ssGDNA	Nano-Au/cMWCNT	264.5 μA/cm^2/ng	Nagraik et al. (2019)
5.	Amperometric DNA sensor for *Salmonella enterica*	*Stn* gene	cMWCNT/AuNP	728.42 (μA/cm^2)/ng	Saini et al. (2019)
6.	Amperometric DNA sensor for scrub typhus	*56 kDa TSA* gene	AuNPs/CNF	7849 (μA/cm^2)/ng	Present method

Au gold, *AuNPs* gold nanoparticles, *cMWCNT* carboxylated multiwalled carbon nanotubes, *CNF* carbon nanofibers, *MOD* mercaptooctadecane, *ssGDNA* single stranded genomic DNA, *RHD* rheumatic heart disease

modified carbon nanofiber-based sensing platform for detection of biological components and revealed their potential application in the designing and fabrication of electrochemical sensors (Mohanaraj et al. 2019; Wang et al. 2012).

In this work, Methylene blue was used as a redox indicator dye to monitor the hybridization event on the transducer surface (working electrode) and convert them into valuable signals during electrochemical studies. The change in I_p values was monitors to analyze the samples (ssGDNA of *O. tsutsugamushi*) on the working electrode surface (AuNPs/CNF) modified with ssDNA probe complementary to the targeted gene (*56 kDa tsa*). Immobilization of the ssDNA probe onto the working electrode (transducer) surface is an essential step in the fabrication of electrochemical DNA sensor. A strong binding and a good orientation are required for immobilization of DNA probe onto the transducer surface for its stable response and higher reactivity. Several methods have been employed for the immobilization of DNA probes such as covalent bonding, adsorption, and Avidin biotin interaction (Yuce and Kurt 2017). Among all methods, covalent bonding is very strong and used in most of the studies for immobilization of DNA probes onto the transducer surface (Asal et al. 2019). So the present method used the carbodiimide cross-linking (EDC-NHS) chemistry, mostly used covalent bonding method for immobilization of DNA probe. The 1-ethyl-3-(3 dimethyl aminopropyl) carbodiimide (EDC) and *N*-hydroxysuccinimide (NHS) are zero-length cross linkers, that make covalent attachment between the carboxyl group and amines (NH2) terminated DNA probe (Rashid and Yusof 2017). Our aim is to develop an approach which is highly specific and sensitive for detection of scrub typhus with less response time and cost. Present method describes use of gold nanoparticles modified carbon nanofibers (AuNPs/CNF)-based screen printed electrode (working electrode) modified with ssDNA probe using carbodiimide cross-linking (EDC-NHS) chemistry for the early and rapid detection of scrub typhus infection using patient samples (Fig. 1).

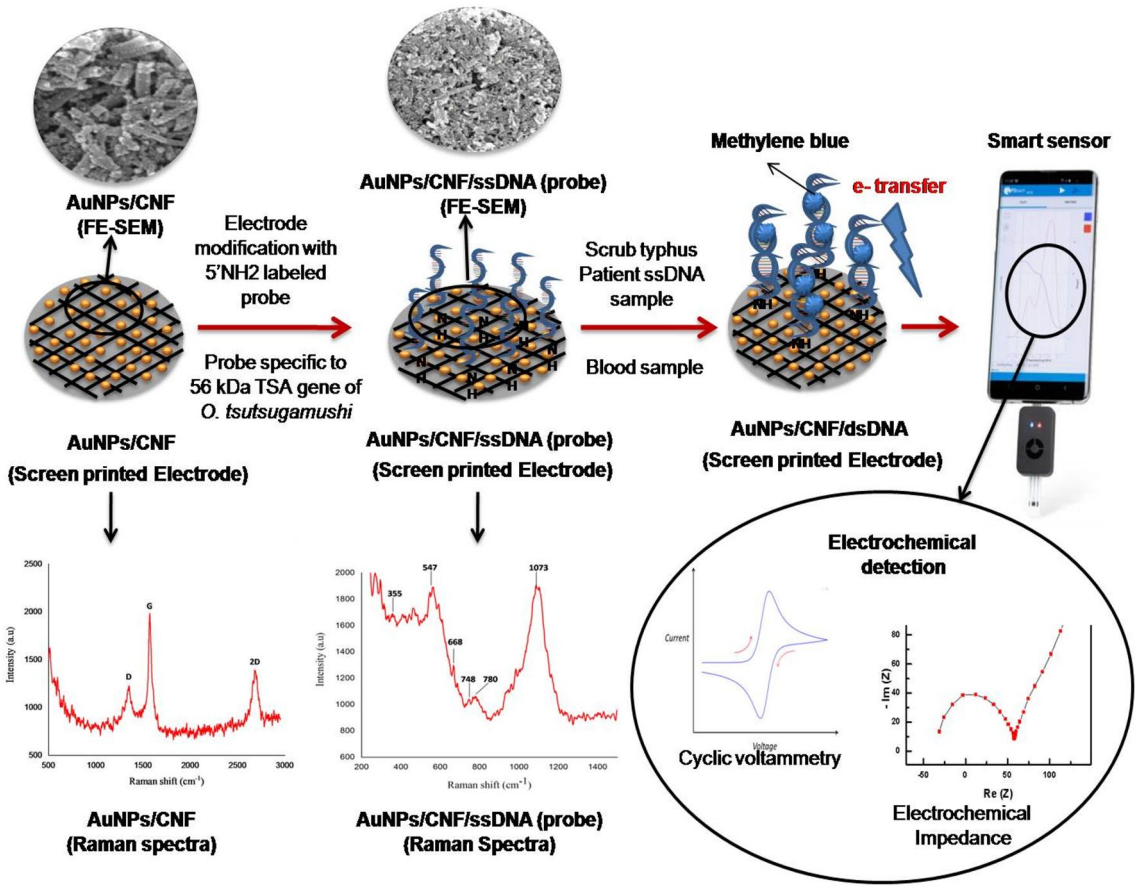

Fig. 1 Schematic representation of electrochemical DNA biosensor fabrication process along with their characterization methods at each step of electrode modification

Experimental methods

Materials

N-Hydroxysuccinimide (NHS), 1-ethyl-3-(3-dimethylaminopropyl) carbodiimide (EDC), methylene blue (MB), were obtained from Sigma Aldrich, USA. Ethanol, hydrochloric acid, sodium chloride, Potassium di-hydrogen phosphate, *di*-sodium hydrogen orthophosphate, tris (hydroxymethyl) aminomethane (Tris), ethylenediamine-tetraaceticacid (EDTA) and other chemicals were received from Qualigens, India. 5′-Amine modified ssDNA probe 20 mer (5′NH_2-GCAATG TCTGCGTTGTCGTT-3′) of *56 kDa TSA* gene was synthesized from Eurofins Genomics India Pvt. Ltd.

Instruments used

Potentiostat/Galvanostat (Product: Palmsens, model: Palmsens 4, manufactured by Palmsens, The Netherland). Screen printed Gold nanoparticles modified carbon nanofiber-based screen printed electrodes (Order no: 110CNF-GNP) were purchased from Dropsens, Spain and working electrode surface was modified at Amity University, Haryana. Field-Emission Scanning electron microscope (FE-SEM) (Make: JFEI company Of USA (S.E.A.) PTE LTD, Model: Nova Nano SEM-450). Nanodrop Spectrophotometer (Make: QIAGEN, Germany, model: QIAXPERT), Fourier transform infrared spectrometer (Perkin Elmer, Frontier), Raman spectrophotometer (ANDOR, SR-500i-B2) of 656 nm wavelength laser was used. Double distilled water (DW) for reagent preparation and milli Q water for DNA was used throughout the experimental studies.

Isolation of DNA from patient samples

The genomic DNA was isolated from patient's Blood samples using QIAamp DNA Mini Kit. The different concentrations of isolated DNA were prepared and denatured to ssDNA at 95 °C for 5 min followed by hybridization with ssDNA probe on working electrode surface (AuNPs/CNF/ssDNA $_{(probe)}$) for 10 min at room temperature (25 ± 3 °C). Genomic DNA (G-DNA) from other bacterial cultures (*Salmonella enterica, Klebsiella pnuemoniae* and *Leptospira interrogans*) was also isolated to check specificity of fabricated DNA biosensor.

Construction and response measurement of DNA biosensor for detection of Scrub Typhus

AuNPs/CNF-based DNA biosensor was constructed using ssDNA probe specific to 56 kDa TSA gene of *O. tsutsugamushi*. Screen printed electrode consist of AuNPs/CNF as working electrode, carbon as counter electrode and silver as a reference electrode. The working electrode was modified with equimolar amount (10 mM each) of EDC: NHS (1:1, v/v) in 1xPBS buffer (0.137 M NaCl, 0.0027 M KCl, Na_2HPO_4, 0.01 M, 0.0018 KH_2PO_4), pH 7.4 for 1.3 h, to activate the –COOH groups on the surface. After activation, electrode surface was washed with PBS buffer (pH 7.4) to remove excess of the reagents and air dried at room temperature (25 ± 3 °C).

5′-NH_2 modified ssDNA Probe (10 pmol) in TE buffer (10 mM Tris, 1 mM EDTA), pH 8 was added onto the activated AuNPs/CNF working electrode surface for overnight to form the amide bond between –COOH group of AuNPs/CNF and –NH_2 group of ssDNA probe results in construction of AuNPs/CNF/ssDNA$_{(probe)}$-based working electrode. The immobilization step was followed by washing with TE buffer (pH 8.0) to remove unbound ssDNA probe and dried at room temperature (25 ± 3 °C). Different dilutions of single stranded genomic DNA (ssG-DNA) 0.04–2.6 ng was prepared in TE buffer (10 mM Tris, 1 mM EDTA), pH 8 and hybridized with AuNPs/CNF/ssDNA $_{(probe)}$-based electrode for 10 min at room temperature ((25 ± 3 °C). in moisturized chamber. The hybridization step was followed by washing step using TE buffer (10 mM Tris, 1 mM EDTA), pH 8. Cyclic voltammetry (CV) and electrochemical impedance (EI) was recorded in Potentiostat/Galvanostat including 50 µl of methylene blue and 1 mM [K_3 Fe(CN)$_6$] in pH 7.4, PBS buffer.

Characterization of DNA biosensor

The electrochemical DNA biosensor was characterized using Field-Emission Scanning electron microscopy (FE-SEM), Fourier transform infrared spectroscopy (FTIR) and Raman spectroscopy. Characterization studies were performed to compare the fabrication steps of electrochemical DNA biosensor including bare electrode, immobilized ssDNA probe and hybridized cDNA of *O. tsutsugamushi.* The FE-SEM study was performed to monitor the morphological changes on electrode surface after immobilization of ssDNA probe and hybridization of cDNA. FTIR and Raman study reveals about functional groups imparted onto the surface of AuNPs/CNF electrode after immobilization of DNA probe.

Optimization of DNA biosensor

Optimization studies of electrochemical DNA biosensor was performed to find out the optimum conditions (pH, incubation time and analyte concentration) required for higher output of sensor. The pH was varied in between pH 5–9 at an interval of pH 1.0 to determine the effect of pH on hybridization efficiency using sodium phosphate buffer (pH

5–7), Tris–HCL EDTA buffer (pH 8–9). Similarly optimum hybridization time was calculated at different time intervals (1–15 min) and linearity of biosensor response was checked with different concentration of G-DNA (0.04–10 ng).

Specificity study

Specificity of developed electrochemical DNA biosensor was checked with isolated G-DNA of *O. tsutsugamushi* and other similar bacteria causing monsoon disease (*L. interrogans, S. enterica, K. pnuemoniae*). The qualitative and quantitative estimation of isolated DNA samples were performed using nanodrop spectrophotometer. The isolated DNA samples were heated at 95 °C for 5 min and hybridize with AuNPs/CNF/ssDNA $_{(probe)}$ working electrode. The response of DNA biosensor for different bacterial DNA samples (same concentration) was recorded using cyclic voltammetry and change in peak current (I_p) with respect to probe (control) was measured to determine the specificity of DNA biosensor.

Selectivity study

Selectivity of electrochemical DNA biosensor against complementary DNA sequence was evaluated using different mismatched bases in DNA sequence (Table 2). Selectivity of the sensor was calculated based on percentage of CV current (% I_p *nc*DNA) using the following equation:

$$\% \, I_p ncDNA = \left({}^{I_p ncDNA}/_{I_p cDNA} \right) \times 100\% \, , \quad (1)$$

where I_p *nc*DNA and I_p *c*DNA are peak currents of hybridized DNA probe with mismatched DNA base and complementary DNA, respectively.

Table 2 Oligonucleotide sequence of DNA probe and cDNA containing different number of mismatched bases used in present study

DNA sample	Base sequence
DNA Probe	5′GCAATGTCTGCGTTGTCG TT 3′
Control (cDNA)	5′AACGACAACGCAGACATT GC 3′
1 base mismatched DNA	5′TACGACAACGCGGACATT GC 3′
2 base mismatched DNA	5′TGCGACAACGCGGACATT GC 3′
3 base mismatched DNA	5′TGTGACAACGCGGACATT GC 3′
Multiple base mismatched DNA	5′TGTAGTAACATGAACATT AC 3′

Regeneration of electrochemical DNA biosensor

Regeneration capability of electrochemical DNA biosensor was evaluated using 0.1 mM HCl solution. Acidic HCl solution breaks down the hydrogen bonds between DNA probe-cDNA and converts them in single stranded form. However, prolonged exposure to HCl solution causes break down of covalent bonds in between electrode surface and DNA probe, provides a way to reuse an electrode for multiple experiments. DNA probe-cDNA hybridization was performed at room temperature (25 ± 3 °C) for 10 min and 1 mM HCl treatment to the electrode was given for different time period of 60–300 s. The reproducibility of the sensor was evaluated by comparing I_p value of bare electrode with other values obtained after treatment of electrode with 1 mM HCl for different time interval.

Validation study

The developed electrochemical DNA biosensor was validated with GDNA isolated from patient's sample. All collected patient blood samples ($n = 9$) was confirmed with ELISA and further subjected to DNA isolation for their analysis by electrochemical DNA biosensor. The I_p value of AuNPs/CNF/ssDNA (probe) was compared with values obtained from positive control, negative control and sample DNA for validation. All voltammetric readings were taken in triplicate and average value of respective samples and controls were considered for final validation.

Results and discussion

DNA Hybridization response

Figure 2 shows cyclic voltammogram of AuNPs/CNF bare electrode, AuNPs/CNF/ssDNA $_{(probe)}$ and its hybridization with different concentration of cDNA of *O. tsutsugamushi*. The I_p of AuNPs/CNF/double stranded DNA (dsDNA) was higher than AuNPs/CNF/ssDNA $_{(probe)}$ and concurrently increased with higher concentration of complementary G-DNA. Methylene blue was used as redox indicator dye which monitors the hybridization event on the transducer surface and converts them into valuable signals during electrochemical studies. The change in I_p values is due to the electrostatic interaction of methylene blue (MB) with exposed nitrogenous bases (guanine bases), which is minimum in bare electrode than AuNPs/CNF/ssDNA$_{(probe)}$ and AuNPs/CNF/dsDNA. The ssDNA probe contains limited number of exposed nitrogenous bases as compare to the exposed unhybridized single stranded genomic DNA (ssG-DNA) onto the transducer surface after probe-cDNA hybridization. Unhybridized ssDNA sequence contains

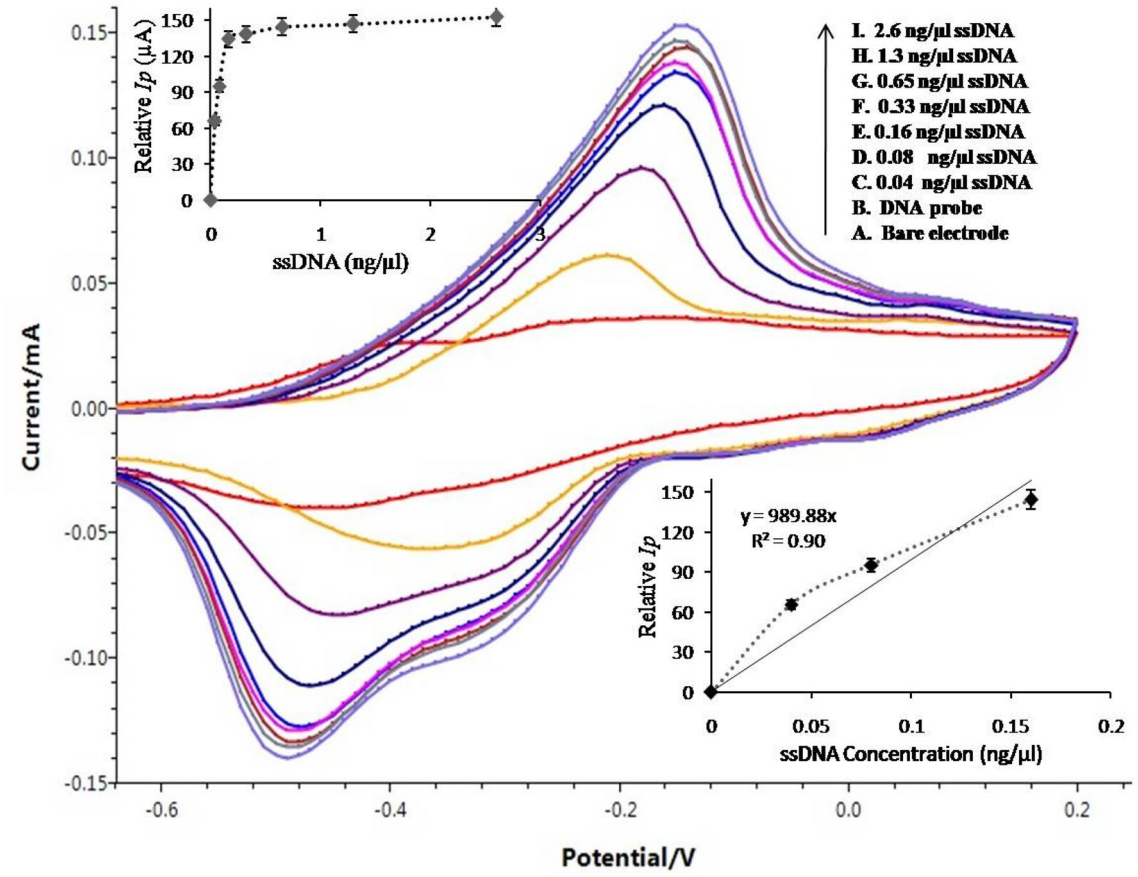

Fig. 2 Cyclic voltammogram of (A) AuNPs/CNF electrode, (B) AuNPs/CNF/ssDNA$_{(probe)}$ and (C–I) hybridization with different concentration of ssG-DNA of *Orientia tsutsugamushi*. The experiment was conducted using 1 mM methylene blue as a redox indicator with a potential range of − 0.6 V to 0.2 V and scan rate of 30 mV/s

numerous nitrogenous bases which binds more MB molecules through electrostatic binding (Lin et al. 2014, 2015) leading to increase in the I_p value. The average of three I_p values was plotted against ssG-DNA concentrations with respect to probe (zero), that forms hyperbolic curve and relative current values also show linearity from 0.04–2.6 ng ssG-DNA with a regression coefficient of (R^2) 0.90. The sensitivity (S) of DNA sensor was calculated using the formula $S = m/A$, where m is the slope of the linear equation, and A is the area of the working electrode (0.126 cm^2). The LOD of the DNA sensor was calculated using the formula LOD = 3 (σ/S), where σ is the standard deviation and S is the sensitivity. The sensitivity of the electrochemical DNA biosensor was 7849 (µA/cm^2)/ng DNA and LOD was calculated as 0.02 ng/µl of ssDNA.

The reason behind the shifting of the potential in the CV plots of the present study is that the current itself is dependent on the rate at which material gets from the bulk of solution to the electrode, known as mass transport. Diffusion is the random movement of molecules from a region of high concentration to regions of lower concentration. At a low concentration of the analyte, diffusion occurs in a satisfactory way, but at high concentration, the diffusion process is disrupted. In this condition, mass transport will be in trouble, so, to compensate for this problem and re-establishment of mass transport, the electrochemical system applies more potential; therefore, the peak potential will be shifted.

The DNA biosensor was also characterized by electrochemical impedance spectroscopy in a frequency range of 10^{-2}–10^5 Hz using 1 mM [$K_3Fe(CN)_6$] in PBS buffer, pH-7.4. The R_{ct} value of bare AuNPs/CNF electrode was lower than AuNPs/CNF/ssDNA$_{(probe)}$ that indicates faster electron exchange kinetic of $[Fe(CN)_6]^{3-/4-}$ with bare AuNPs/CNF electrode. Increase in R_{ct} value of AuNPs/CNF/ssDNA$_{(probe)}$ resulted from the immobilization of ssDNA probe containing electronegative phosphate group, which prevents $[Fe(CN)_6]^{3-/4-}$ ions to reach the AuNPs/CNF electrode surface (Fig. 3). Furthermore, AuNPs/CNF/ssDNA$_{(probe)}$ was hybridized with different concentrations of complementary ssG-DNA and increase in R_{ct} value were obtained which can be attributed to the increase in negative charges of extra deoxyribose backbone of DNA leading to

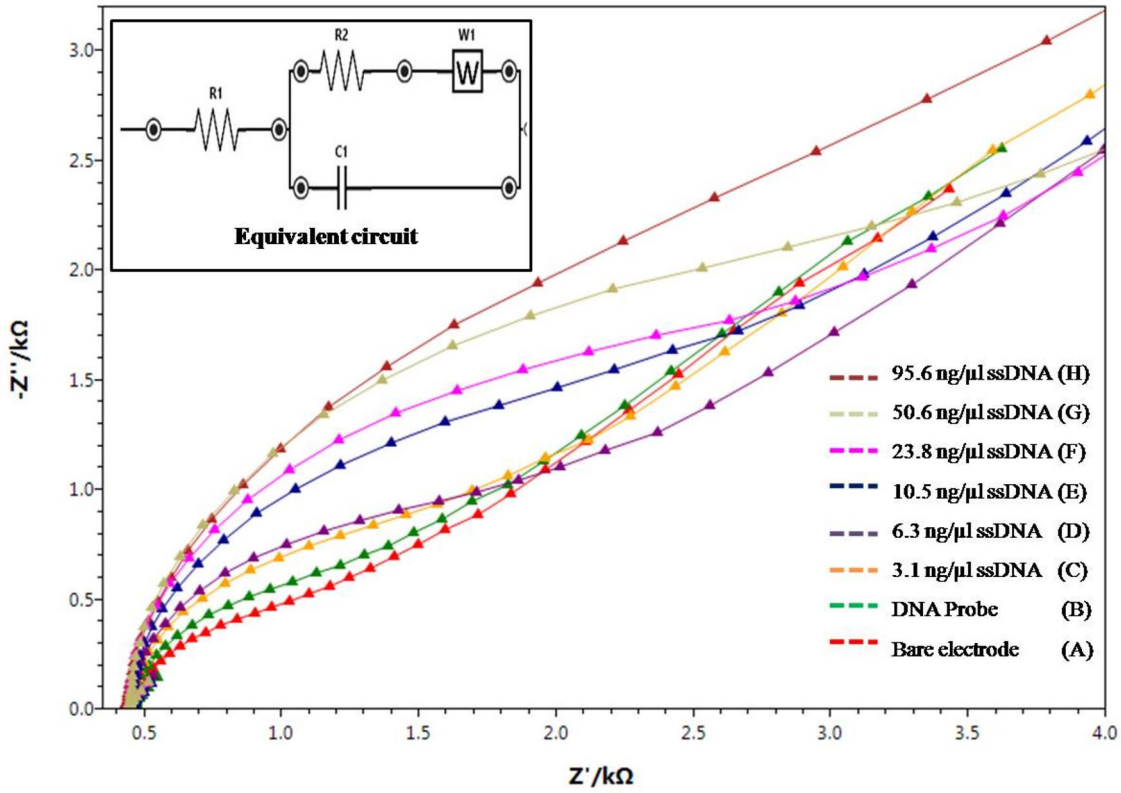

Fig. 3 Characterization of electrochemical DNA chip fabrication steps including (A) Bare electrode surface (AuNPs/CNF), (B) AuNPs/CNF/ssDNA $_{(probe)}$, (C–H) Hybridization with different concentration of ssG-DNA of *Orientia tsutsugamushi*, using electrochemical impedance spectroscopy. Electrochemical impedance studies were performed using 1 mM potassium ferricyanide (in Phosphate buffer saline, pH 8.0) solution. The Impedance values were in increasing order from the bare working electrode (A) to immobilized ssDNA probe modified electrode (B) and subsequently increased with concentrations (C–H) of complementary ss GDNA of *Orientia tsutsugamushi*

increase in repulsion with $[Fe(CN)6]^{3-/4-}$ ions. Impedance was in increasing order from bare electrode to immobilized probe and hybridized complementary DNA that shows the success of electrode fabrication process and DNA hybridization event.

Characterization studies

Electrochemical DNA biosensor was characterized at each step of fabrication using FE-SEM, FTIR and Raman spectroscopy.

The FE-SEM images of the bare AuNPs/CNF electrode, AuNPs/CNF/ssDNA$_{(probe)}$ and AuNPs/CNF/ssDNA$_{(probe)}$ hybridized with complementary G-DNA of *O. tsutsugamushi* is shown in Fig. 4a–c, respectively. All FE-SEM images were taken in magnification of 25,000 × using the accelerating voltage of 500 kV. The morphological changes at each step of electrode modification could be observed clearly from the FE-SEM images. In Fig. 4a of bare AuNPs/CNF electrode, we can observe the fibrous structure of CNFs decorated with AuNPs. In the case of AuNPs/CNF/ssDNA (probe), the covalently immobilized ssDNA probe formed a thin film (Fig. 4b) which changed into a dense surface morphology (Fig. 4c) after hybridization with ssGDNA in the case of AuNPs/CNF/dsDNA.

FTIR analysis was performed to ensure the immobilization of ssDNA probe onto the surface of AuNPs/CNF modified screen printed electrode (Fig. 5). The FTIR spectra in Fig. 5a show transmittance of the bare AuNPs-CNF electrode. In FTIR spectrum transmittance peaks around 777, 1680 and 2512 cm^{-1} indicative of aromatic C–H bending, C=O and O–H stretching. In addition, Fig. 5b shows FTIR spectra of AuNPs-CNF-ssDNA probe exhibits transmittance peaks at 638,734, 1044 and 1182 cm^{-1} corresponding to the C_2=O stretch of thymine, C=O stretch of guanine, in plane vibration of cytosine and C_7=N vibration of adenine, respectively, ensures the presence of 4 nucleotide bases of DNA on the surface. Peaks at 2983 and 1238 cm^{-1} correspond to C–H and PO_2^- stretch of deoxyribose backbone, respectively. The peaks at 1410 and 1558 cm^{-1} are corresponding to C–O–H and CO–NH (amide bond), respectively. The peaks show

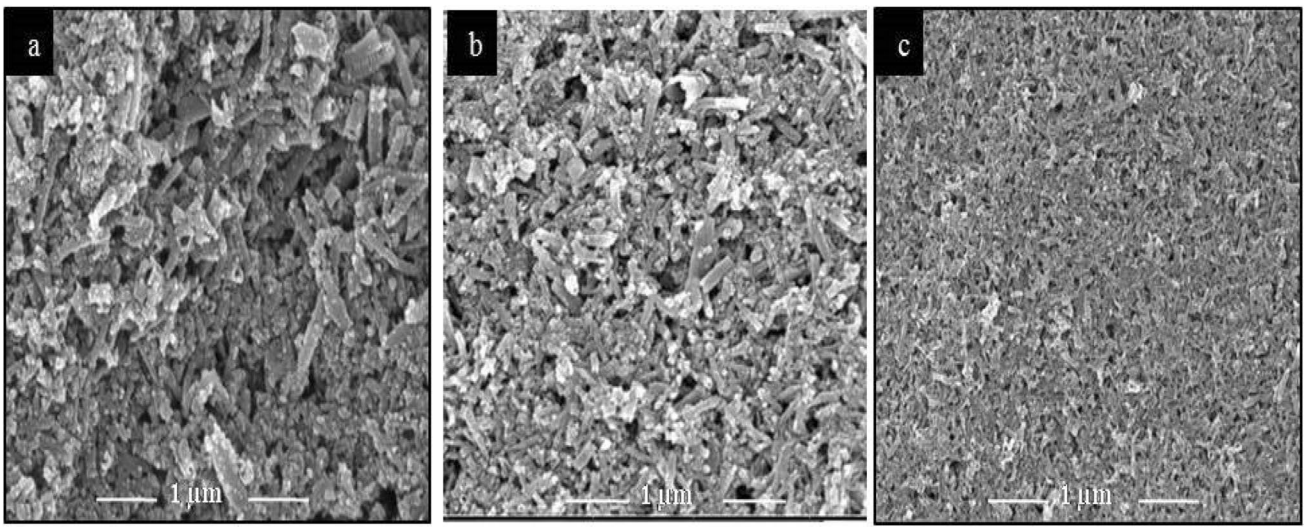

Fig. 4 FE-SEM micrograph of different steps of electrode modifications including **a** bare screen printed AuNPs/CNF electrode, **b** ssDNA Probe modified AuNPs/CNF electrode, and **c** hybridization with complementary ssDNA

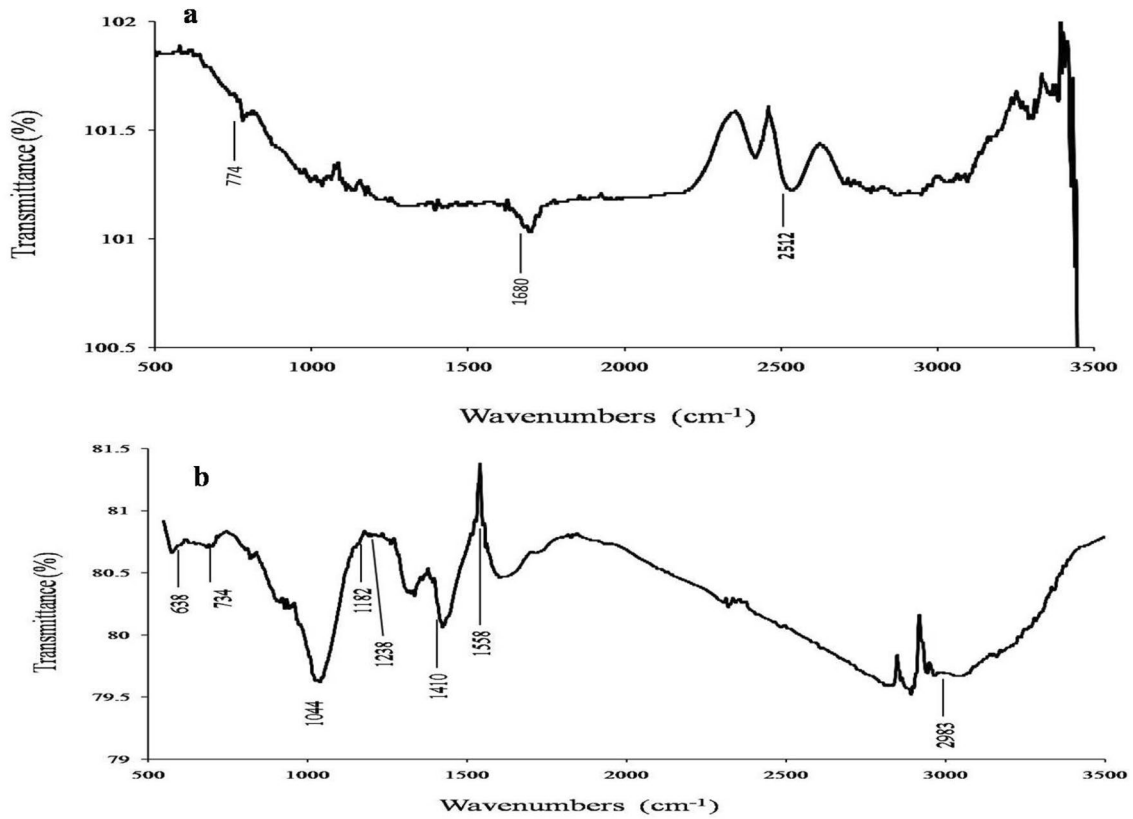

Fig. 5 FTIR spectra of **a** AuNPs-CNF and **b** AuNPs-CNF-ssDNA at frequency range of 500–3500 cm^{-1} ensures the immobilization of ssDNA probe onto the surface of AuNPs-CNF electrode

the carbodiimide cross-linking of NH_2 group of the probe with –COOH group on the electrode surface.

Furthermore, the electrode surface was characterized by Raman spectroscopy (Suppl. Fig. S1) to ensure the DNA immobilization process. The Raman shift was in agreement with the FTIR spectra and shows the peaks at around 355 & 547 cm^{-1} (vibration of adenine), 668 cm^{-1} (vibration of T; G; A), 780 cm^{-1} (vibration of cytosine) and 1073 cm^{-1}

(vibration of PO_2^-) that ensure the immobilization of the ssDNA probe onto the bare electrode surface. The graphitization pattern also appeared on bare working electrode surface as the peak appears at 1277, 1566, 2660 cm^{-1} corresponds to D, G and 2D bands of graphene-based materials.

Optimization of electrochemical DNA biosensor response

The developed nanosensor was optimized at different pH conditions, hybridization time and analyte concentrations. The highly acidic and alkaline solution can damage the electrode surface as well as can reduce DNA solubility and hybridization rate. In the present study the biosensor shows the maximum response for DNA hybridization at pH 8.0. Furthermore, the incubation time for DNA hybridization was optimized as 10 min as maximum I_p value was obtained till this point and become constant in subsequent incubation time periods. The incubation for ssDNA-Probe hybridization was performed at room temperature (25 ± 3 °C) and no effect on I_p values was observed by changing incubation temperature from 7 to 28 °C. Hence the electrochemical biosensor response was found linear in the range of 0.04–2.6 ng ssDNA and the current shows saturation after this value as current becomes constant after this point.

Performance of electrochemical DNA biosensor

The performance of electrochemical DNA biosensor was evaluated in context of specificity, selectivity and restoration competency.

The specificity of the developed electrochemical DNA biosensor with *O. tsutsugamushi* and other similar bacteria causing monsoon disease (*L. interrogans, S. enterica, K. pnuemoniae,*) is shown in Fig. 6. After hybridization increase in I_p value with respect to probe was observed only with *O. tsutsugamushi,* whereas other samples show inconsiderable changes in I_p value after hybridization. The sensor specificity was evaluated at 10 ng/µl DNA concentration for all organisms. The increase in I_p value only in case of *O. tsutsugamushi* confirms the specificity of the sensor towards the targeted organism and overcome the specificity

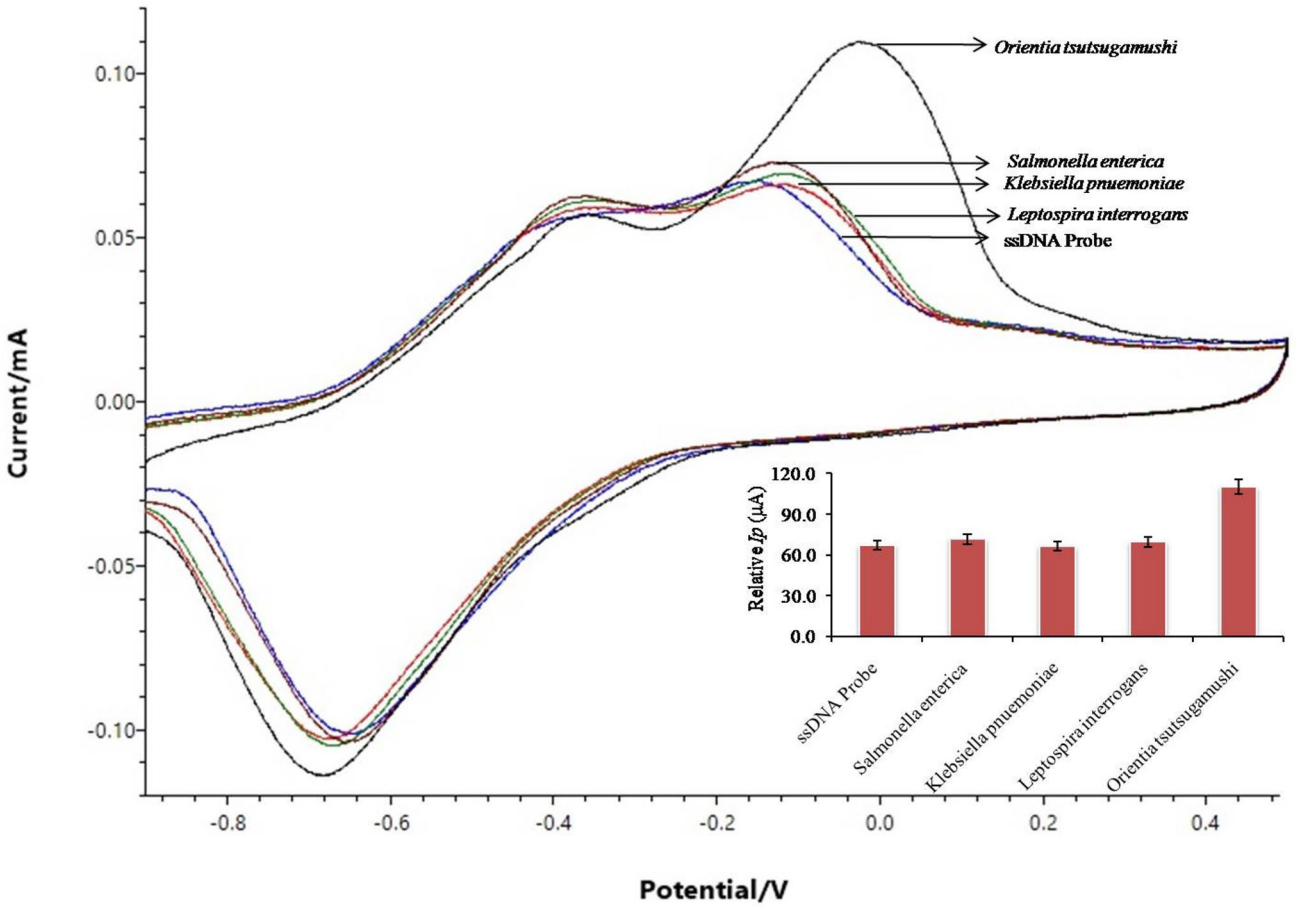

Fig. 6 Specificity of electrochemical DNA chip with GDNA of *O. tsutsugamushi* and other similar bacteria causing monsoon disease (*L. interrogans, S. enterica, K. pnuemoniae*)

Table 3 Percent CV peak current of Probe hybridization with complementary DNA and DNAs containing different number of mismatched bases

DNA Sample	Peak current (μA)	Peak current of DNA (%)
Control (cDNA)	30.96	100
1 base mismatched DNA	18.43	59.53
2 base mismatched DNA	15.93	51.45
3 base mismatched DNA	13.43	43.38
Multiple base mismatched DNA	4.43	14.31

issues of other diagnosis methods used for the detection of scrub typhus. Our study confirms that the electrochemical DNA biosensor is highly specific to *56 kDa TSA* gene of *O. tsutsugamushi* and shows higher efficiency of binding to the complementary site only, as no binding efficiency was observed with other organism's DNA samples. The electrochemical DNA biosensor shows a significant limit of detection (0.02 ng/μl), sensitivity [7849 (μA/cm^2)/ng DNA] and specificity for *O. tsutsugamushi.*

In selectivity study percentage CV peak current of Probe hybridization with mismatched DNA sequences were compared with complementary DNA. The selectivity of electrochemical DNA biosensor was found higher for complementary DNA sequence as compared to mismatched base DNA sequences (Table 3). The CV peak current (I_p) percentages of probe hybridization with one, two and three-base mismatched DNAs were 59.5%, 51.4% and 43.3%, respectively, and probe hybridization with multiple base mismatched DNA shows a downfall in peak current to 14.3% relative to cDNA (Suppl. Fig. S2). The biosensor response towards the mismatched DNA sequences was found declining with increased mismatched bases and found equivalent to non-complementary DNA sequences with multiple mismatch bases.

Restoration competency of electrochemical DNA sensor was evaluated by treating the ss GDNA hybridized AuNPs/CNF/ssDNA$_{(probe)}$ electrode with 1 mM HCl solution. The I_p value was measured before and after treatment of the electrode with 1 mM HCl solution at different dipping time (60–300 s). The biosensor response was declined after treating electrode with 1 mM HCl due to the denaturation of ssDNA-Probe complex. The biosensor response after treatment of 1 mM HCl from 60 to 300 s with a time interval of 60 s were 17.7, 9.64, 9.54, 8.4 and 4.64 μA, respectively, with respect to initial biosensor response (Suppl. Fig. S3).

Validation of AuNPs/CNF-based sensor

The electrochemical DNA biosensor was validated using ELISA positive patient blood samples collected from MMU, Solan, India (Table 4). The DNA was isolated from patients sample using QIAamp DNA Mini Kit and further subjected to electrochemical study for validation. The change in CV peak current (I_p) with respect to DNA probe, negative control (Human GDNA) and positive control (GDNA of *O. tsutsugamushi*) analysed to validate the patient samples. The patient samples (6 μl ssDNA) were hybridized with AuNPs/CNF/ssDNA probe and CV peak current (I_p) was recorded and compared with the I_p of negative control and positive control for sample validation (Fig. 7). Total 9 ELISA positive blood samples were analysed and all were found positive using electrochemical DNA biosensor. Our biosensor shows a better correlation with the ELISA method and able to detect the infection with more sensitivity and in less time. So the developed sensor is efficient than ELISA and PCR in context of specificity, sensitivity and response time. The biosensor is able to detect the infection at early stages that is not possible with current available diagnostic methods like ELISA, IFA and ICT.

Table 4 Details of scrub typhus patients samples used for validation of DNA biosensor

Sample ID	Age	Sex	ELISA response	DNA biosensor response
S_1	30	F	+ve	+ve
S_2	23	M	+ve	+ve
S_3	24	F	+ve	+ve
S_4	27	F	+ve	+ve
S_5	39	F	+ve	+ve
S_6	25	F	+ve	+ve
S_7	62	M	+ve	+ve
S_8	35	F	+ve	+ve
S_9	27	M	+ve	+ve

+ve positive sample, *F* female, *M* male

Conclusion

An electrochemical DNA biosensor for detection of scrub typhus based on AuNPs/CNF electrode modified with DNA probe specific for *56 kDa TSA* gene was successfully fabricated. The biosensor shows better performance in terms of faster response time (60 s), wider linearity (0.04–2.6 ng), and lower limit of detection (0.02 ng) with higher specificity. The AuNPs/CNF-based sensor shows excellent sensitivity as the sensor is able to sense even lower concentrations of *O. tsutsugamushi* G-DNA. The higher selectivity and affinity of bioreceptors (DNA probe) towards the *56 KDA TSA* gene of *O. tsutsugamushi* improves the LOD of the developed sensor. The sensitivity of the DNA biosensor is further enhanced by the use of

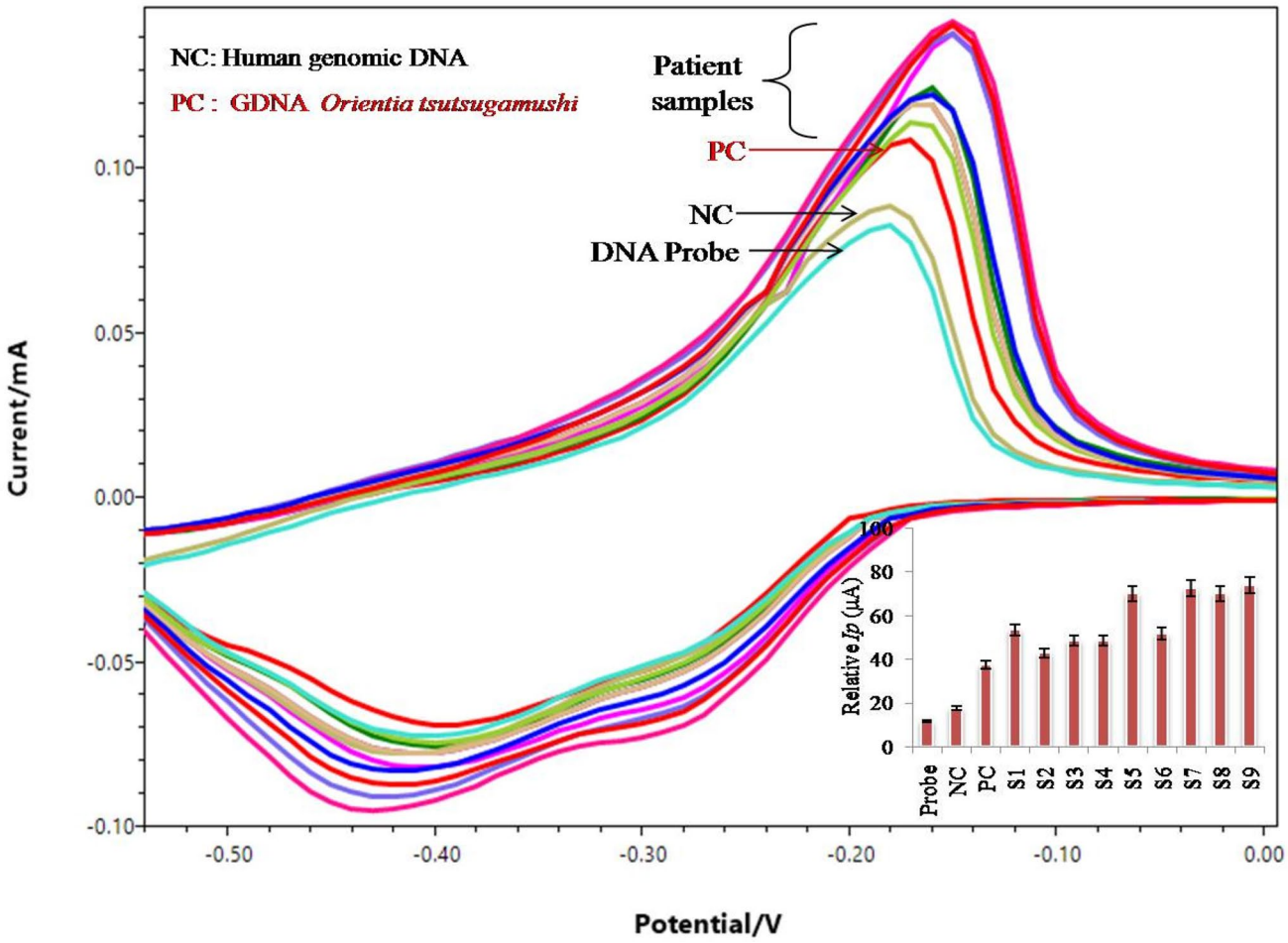

Fig. 7 Validation of the electrochemical DNA chip with 9 ELISA positive scrub typhus patient blood DNA samples using positive control (PC) and negative control (NC)

AuNPs/CNF nanocomposite modified transducer (working electrode), which provides the larger surface area for immobilization of bioreceptors and larger electrochemical active area to work on a lower current range that will be beneficial for detection of the patients samples with lower recovery of *O. tsutsugamushi* G-DNA. Furthermore, the developed sensor is a portable device which can be used in remote areas for better monitoring of the infection without any requirement of trained staff and sophisticated laboratory facility. The developed sensor overcomes the sensitivity, specificity and selectivity issues of other diagnostic methods. No such biosensor has been reported till now and can become a future point of care system for diagnosis of scrub typhus.

Acknowledgements This work was supported by Department of Science and Technology, (DST), Govt. of India (SP/YO/079/2017). We would also like to show our gratitude to Dr. Amisha Sharma, Head Department of Microbiology, MMMC&H, Solan, H. P. for providing patient's DNA sample to carry out the research work.

Author contributions The first author and the corresponding author contributes major part in the manuscript. All the other authors have contributed equally to the manuscript.

Compliance with ethical standards

Conflict of interest The authors declare that they have no conflict of interest in the publication.

References

Asal M, Ozen O, Sahinler M, Baysal HT, Polatoglu I (2019) An overview of biomolecules, immobilization methods and support materials of biosensors. Sens Rev 39:377–386. https://doi.org/10.1108/SR-04-2018-0084

Baby TT, Aravind SJ, Arockiadoss T, Rakhi RB, Ramaprabhu S (2010) Metal decorated graphene nanosheets as immobilization matrix for amperometric glucose biosensor. Sens Actuat B-Chem 145:71–77. https://doi.org/10.1016/j.snb.2009.11.022

Biswal M, Zaman K, Suri V, Rao H, Kumar A, Kapur G, Sharma N, Bhalla A, Jayashree M (2018) Use of eschar for the molecular diagnosis and genotypic characterisation of *Orientia*

tsutsugamushi causing scrub typhus. Indian J Med Microbiol 36:422–425. https://doi.org/10.4103/ijmm.ijmm_18_8

Blacksell SD, Luksameetanasan R, Kalambaheti T, Aukkanit N, Paris DH, McGready R, Nosten F, Peacock SJ, Day NP (2008) Genetic typing of the 56-kDa type-specific antigen gene of contemporary *Orientia tsutsugamushi* isolates causing human scrub typhus at two sites in north-eastern and western Thailand. FEMS Immunol Med Microbiol 52:335–342. https://doi.org/10.1111/j.1574-695x.2007.00375.x

Bonell A, Lubell Y, Newton PN, Crump JA, Paris DH (2017) Estimating the burden of scrub typhus: a systematic review. Plos Negl Trop Dis 11:e0005838. https://doi.org/10.1371/journal.pntd.0005838

Chunchanur SK (2018) Scrub typhus in India- an impending threat. Ann Clin Immunol Microbiol 1:1003

Dash SK, Sharma M, Khare S, Kumar A (2014) Carbon-mercaptooctadecane/carboxylated multi-walled carbon nanotubes composite based genosensor for detection of bacterial meningitis. Indian J Microbiol 54:170–177. https://doi.org/10.1007/s12088-013-0435-7

Hu Y, Hua S, Li F, Jiang Y, Bai X, Li D, Niu L (2011) Green-synthesized gold nanoparticles decorated graphene sheets for label-free electrochemical impedance DNA hybridization biosensing. Biosens Bioelectron 26:4355–4361. https://doi.org/10.1016/j.bios.2011.04.037

Huang J, Liu Y, You T (2010) Carbon nanofiber based electrochemical biosensors: a review. Anal Methods 2:202–211. https://doi.org/10.1039/b9ay00312f

Kala D, Gupta S, Nagraik R, Verma V, Thakur A, Kaushal A (2020) Diagnosis of scrub typhus: recent advancements and challenges. 3 Biotech 10:396. https://doi.org/10.1007/s13205-020-02389-w

Kaushal A, Singh S, Kala D, Kumar D, Kumar A (2016) *SpeB* genosensor for rapid detection of *Streptococcus pyogenes* causing damage of heart valves in human. Cell Mol Biol 62:140

Kaushal A, Singh S, Kumar A, Kumar D (2017) Nano-Au/cMWCNT modified speB gene specific amperometric sensor for rapidly detecting *Streptococcus pyogenes* causing rheumatic heart disease. Indian J Microbiol 57:121–124

Kelly DJ, Fuerst PA, Ching WM, Richards AL (2009) Scrub typhus: the geographic distribution of phenotypic and genotypic variants of *Orientia tsutsugamushi*. Clin Infect Dis 48:S203–S230. https://doi.org/10.1086/596576

Koh GC, Maude RJ, Paris DH, Newton PN, Blacksell SD (2010) Diagnosis of scrub typhus. Am J Trop Med Hyg 82:368–370. https://doi.org/10.4269/ajtmh.2010.09-0233

Lee IY, Kim HC, Sun Lee Y, Seo JH, Lim JW, Yong TS, Klein TA, Lee WJ (2009) Geographical distribution and relative abundance of vectors of scrub typhus in the Republic of Korea. Korean J Parasitol 47:381–386. https://doi.org/10.3347/kjp.2009.47.4.381

Li Z, Chen J, Li W, Chen K, Nie L, Yao S (2007) Improved electrochemical properties of prussian blue by multi-walled carbon nanotubes. J Electroanal Chem 603:59–66. https://doi.org/10.1016/j.jelechem.2007.01.021

Lin PR, Tsai HP, Tsui PY, Weng MH, Kuo MD, Lin HC, Chen KC, Ji DD, Chu DM, Liu WT (2011) Genetic typing, based on the 56-kilo dalton type-specific antigen gene of *Orientia tsutsugamushi* strains isolated from chiggers collected from wild-caught rodents in Taiwan. Appl Environ Microbiol 77:3398–3405. https://doi.org/10.1128/aem.02796-10

Lin C, Wu Y, Luo F, Chen D, Chen X (2014) A label-free electrochemical DNA sensor using methylene blue as redox indicator based on an exonuclease III-aided target recycling strategy. Biosens Bioelectron 59:365–369. https://doi.org/10.1016/j.bios.2014.03.053

Lin X, Yongnian N, Serge K (2015) An electrochemical DNA-sensor developed with the use of methylene blue as a redox indicator for the detection of DNA damage induced by endocrine-disrupting compounds. Anal Chim Acta 867:29–37. https://doi.org/10.1016/j.aca.2015.02.050

Mohanaraj S, Wonnenberg P, Cohen B, Zhao H, Hartings MR, Zou S, Fox DM, Zestos AG (2019) Gold nanoparticle modified carbon fiber microelectrodes for enhanced neurochemical detection. J Vis Exp 13:147. https://doi.org/10.3791/59552

Nagraik R, Kaushal A, Gupta S, Dhar P, Sethi S, Kumar D (2019) Optimized DNA-based bioassay for Leptospira interrogans detection: a novel platform for leptospirosis diagnosis. 3 Biotech 9:284. https://doi.org/10.1007/s13205-019-1815-4

Paris DH, Shelite TR, Day NP, Walker DH (2013) Unresolved problems related to scrub typhus, a seriously neglected life-threatening disease. Am J Trop Med Hyg 89:301–307. https://doi.org/10.4269/ajtmh.13-0064

Phetsouvanh R, Thojaikong T, Phoumin P, Sibounheuang B, Phommasone K, Chansamouth V, Lee SJ, Newton PN, Blacksell SD (2013) Inter and intra-operator variability in the reading of indirect immunofluorescence assays for the serological diagnosis of scrub typhus and murine typhus. Am J Trop Med Hyg 88:932–936. https://doi.org/10.4269/ajtmh.12-0325

Prakash JAJ (2017) Scrub typhus: risks, diagnostic issues, and management challenges. Res Rep Trop Med 8:73–83. https://doi.org/10.2147/rrtm.s105602

Premaratna R, Blanton LS, Samaraweera DN, de Silva GNN, Chandrasena NT, Walker DH, de Silva HJ (2017) Genotypic characterization of *Orientia tsutsugamushi* from patients in two geographical locations in Sri Lanka. BMC Infect Dis 17:67. https://doi.org/10.1186/s12879-016-2165-z

Rashid JIA, Yusof NA (2017) The strategies of DNA immobilization and hybridization detection mechanism in the construction of electrochemical DNA sensor: a review. Sens Biosens Res 16:19–31. https://doi.org/10.1016/j.sbsr.2017.09.001

Rodkvamtook Wuttikon, Areerate TR, Gaywee J, Richards AL, Jeamwattanalert P, Bodhidatta D, Sangjun N, Prasartvit A, Jatisatienr A, Jatisatienr C (2011) Isolation and characterization of *Orientia tsutsugamushi* from rodents captured following a scrub typhus outbreak at a military training base, Bothong district, Chonburi province, central Thailand. Am J Trop Med Hyg 84:599–607. https://doi.org/10.4269/ajtmh.2011.09-0768

Saini K, Kaushal A, Gupta S, Kumar D (2019) Rapid detection of Salmonella enterica in raw milk samples using Stn gene-based biosensor. 3 Biotech 9:425. https://doi.org/10.1007/s13205-019-1957-4

Saraswati K, Day NP, Mukaka M, Blacksell SD (2018) Scrub typhus point-of-care testing: a systematic review and meta-analysis. Plos Negl Trop Dis 12:e0006330. https://doi.org/10.1371/journal.pntd.0006330

Saraswati K, Phanichkrivalkosil M, Day NP, Blacksell SD (2019) The validity of diagnostic cut-offs for commercial and in-house scrub typhus IgM and IgG ELISAs: a review of the evidence. Plos Negl Trop Dis 13:e0007158. https://doi.org/10.1371/journal.pntd.0007158

Shivalli S (2016) Diagnostic evaluation of rapid tests for scrub typhus in the Indian population is needed. Infect Dis Poverty 5:1–40. https://doi.org/10.1186/s40249-016-0137-6

Singh S, Kaushal A, Khare S, Kumar A (2014) Mga genosensor for early detection of human rheumatic heart disease. Appl Biochem 173:228–238. https://doi.org/10.1007/s12010-014-0836-z

Singh S, Kaushal A, Gautam H, Gupta S, Kumar A (2017a) Ultrasensitive nanohybrid DNA sensor for detection of pathogen to prevent damage of heart valves. Sens Actuator B-Chem 246:300–304. https://doi.org/10.1016/j.snb.2017.02.043

Singh S, Kaushal A, Khare S, Kumar A (2017b) DNA biosensor based sensor for amperometric detection of infectious pathogens. Int J Biol Macromol 103:355–359. https://doi.org/10.1016/j.ijbiomac.2017.05.041

Song YZ, Zhu AF, Zhong H, Song Y, Wu FY, Yang WL, Huang H (2011) Gold nanoparticle/single-walled carbon nanotube film on the surface of glassy carbon electrode and its application. Mater Lett 65:3612–3614. https://doi.org/10.1016/j.matlet.2011.06.031

Ulianas A, Heng LY, Ahmad M, Lau HY, Ishak Z, Ling TL (2014) A regenerable screen-printed DNA biosensor based on acrylic microsphere–gold nanoparticle composite for genetically modified soybean determination. Sens Actuator B-Chem 190:694–701. https://doi.org/10.1016/j.snb.2013.09.040

Usha K, Kumar E, Kalawat U, Kumar BS, Chaudhury A, Gopal DS (2015) Molecular detection of scrub typhus in Tirupati, Andhra Pradesh, India. J Vector Dis 52:171–174

Usha K, Kumar E, Kalawat U, Kumar BS, Chaudhury A, Gopal DS (2016) Molecular characterization of *Orientia tsutsugamushi* serotypes causing scrub typhus outbreak in southern region of Andhra Pradesh, India. Indian J Med Res 144:597–603

Varghese M, Janardhanan J, Mahajan SK, Tariang D, Trowbridge P, Prakash JAJ, David T, Sathendra S, Abraham OC (2015) Molecular epidemiology and genetic diversity of *Orientia tsutsugamushi* from patients with scrub typhus in 3 regions of India. Emerg Infect Dis 21:64–69. https://doi.org/10.3201/eid2101.140580

Wang L, Bo X, Bai J, Zhu L, Guo L (2010) Gold nanoparticles electrodeposited on ordered mesoporous carbon as an enhanced material for nonenzymatic hydrogen peroxide sensor. Electroanalysis 22:2536–2542. https://doi.org/10.1002/elan.201000263

Wang H, Bo X, Ju J, Guo L (2012) Preparation of highly dispersed gold nanoparticles/mesoporous carbon nanofiber composites and their application toward detection of hydrazine. Catal Sci Technol 2:2327–2331. https://doi.org/10.1039/c2cy20300f

Wu Y, Mao X, Cui X, Zhu L (2010) Electroanalytical application of graphite nanofibers paste electrode. Sens Actuator B-Chem 145:749–755. https://doi.org/10.1016/j.snb.2010.01.037

Xu G, Walker DH, Jupiter D, Melby PC, Arcari CM (2017) A review of the global epidemiology of scrub typhus. Plos Negl Trop Dis 11:e0006062. https://doi.org/10.1371/journal.pntd.0006062

Yang HH, Huang IT, Lin CH, Chen TY, Chen LK (2012) New genotypes of *Orientia tsutsugamushi* isolated from humans in Eastern Taiwan. Plos Negl Trop Dis 7:e46997. https://doi.org/10.1371/journal.pone.0046997

Yuce M, Kurt H (2017) How to make nanobiosensors: surface modification and characterisation of nanomaterials for biosensing applications. RSC Adv 78:49386–49403. https://doi.org/10.1039/c7ra10479k

Zhang L, Bi Z, Kou Z, Yang H, Zhang A, Zhang S, Meng X, Zheng L, Zhang M, Yang H, Zhao Z (2015) Scrub typhus caused by *Orientia tsutsugamushi* Kawasaki-related genotypes in Shandong Province, northern China. Infect Genet Evol 30:238–243. https://doi.org/10.1016/j.meegid.2014.12.036

Zheng L, Bi Z, Kou Z, Yang H, Zhang L, Zhao Z (2015) Genotype diversity and distribution of *Orientia tsutsugamushi* in scrub typhus patients and rodents in Shandong, Northern China. Infect Genet Evol 36:126–130. https://doi.org/10.1016/j.meegid.2015.09.008

Zhou M, Shang L, Li B, Huang L, Dong S (2008) Highly ordered mesoporous carbons as electrode material for the construction of electrochemical dehydrogenase-and oxidase-based biosensors. Biosens Bioelectron 24:442–447. https://doi.org/10.1016/j.bios.2008.04.025